Kinetic studies on the formation of acridine-linked DNA triple helices

Keith R. Fox*

Department of Physiology and Pharmacology, University of Southampton, Bassett Crescent East, Southampton, SO16 7PX, UK

Received 1 November 1994

Abstract **We have used DNase I footprinting to measure the rate of intermolecular triple helix formation at the target sites $A_6G_6 \cdot C_6T_6$ and $G_6A_6 \cdot T_6C_6$ with the acridine-linked oligonucleotides Acr-T_5C_5 and Acr-C_5T_5, respectively. Under pseudo first-order reaction conditions we find that the reactions are slow, with half-lives of several minutes. The rates are dependent on the concentration of the third strand oligonucleotide and yield bimolecular association rate constants of 300 $M^{-1} \cdot s^{-1}$ for Acr-T_5C_5 binding to $A_6G_6 \cdot C_6T_6$ and 2000 $M^{-1} \cdot s^{-1}$ for the interaction of Acr-C_5T_5 with $G_6A_6 \cdot T_6C_6$.**

Key words: Triple helix; Association kinetics; DNase I footprinting

1. Introduction

Oligonucleotide-directed triple-helix formation offers the possibility of designing compounds with precise DNA sequence recognition properties which may have application as potential anti-gene agents [1,2]. Two types of triplex motifs have been demonstrated which differ in the orientation of the third strand. Complexes in which the third strand runs parallel to the duplex purine strand are characterised by T·AT and C^+·GC triplets; the third strand is held in place by hydrogen bonds to substituents on the duplex purine strand [3–5]. These triplexes are stabilised by conditions of low pH (<6.0), necessary for protonation of the third strand cytosine. In contrast, antiparallel triplexes are characterised by the formation of A·AT, T·AT and G·GC triplets [6–8], and are stabilised by reverse-Hoogsteen base pairs.

There have been few studies on kinetic aspects of triple helix formation. Early experiments with poly(rA)·2poly(rU) showed that this triplex formed at least 100-times more slowly than the corresponding duplex [9,10]. More recently Maher et al. [11], using a restriction enzyme protection assay, determined that the second order rate constant for binding of a 21 base oligopyrimidine to its duplex target site was about 10^3 $M^{-1} \cdot s^{-1}$. This compares with values of about 10^6 $M^{-1} \cdot s^{-1}$ for duplex formation. Dissociation rate constants for triplexes range between 2×10^{-5} s^{-1} and 2×10^{-4} s^{-1}, depending on the reaction conditions, yielding stable complexes with half-lives in excess of 1 h. These studies, together with others, have revealed several features of the kinetic parameters [12–14]. The association reaction is thought to proceed by a nucleation-zipper reaction, similar to that developed for single strand-to-duplex transitions [15,16]. This nucleation, which corresponds to the formation of 3–5 base triplets, appears to be the rate limiting step in triplex formation.

*Corresponding author. Fax: (44) (703) 594 319.

In this paper we use DNase I footprinting to investigate the rate of formation of complexes between various acridine-linked oligonucleotides and their target sites, which have been cloned into longer DNA fragments. By footprinting the reaction mixture at various times, and measuring the rate of appearance of the footprint, we are able to visualise the association reaction kinetics. The equilibrium binding properties of each triplex have already been described. Acr-T_5C_5 and Acr-C_5T_5 bind to the target sequences $A_5G_5 \cdot C_5T_5$ and $G_5A_5 \cdot T_5C_5$, respectively, at low pH, forming parallel triplexes containing C^+·GC and T·AT triplets [17,18]. We find that in each case the reaction is slow and can be measured on the footprinting timescale.

2. Materials and methods

2.1. Oligonucleotides

Acridine-linked oligonucleotides Acr-T_5C_5 and Acr-C_5T_5 were gifts from Dr. M.J. McLean, Cambridge Research Biochemicals. In these compounds the [2-methoxy, 6-chloro, 9-amino] acridine is linked to the 5′ end of the oligonucleotides by a pentamethylene chain. These were stored at −20°C in water at a concentration of 360 μM.

2.2. Plasmids

The preparation of plasmids containing the inserts $G_6A_6 \cdot T_6C_6$ (pGA1) and $A_6G_6 \cdot C_6T_6$ (pAG1) has been previously described [17,18]. In each case the insert was cloned into the *Sma*I site of pUC18. For pAG1 the insert is oriented so that the purine-containing strand is visualized by labelling the 3′-end of the *Hin*dIII site, whereas for pGA1, containing the insert $G_6A_6 \cdot T_6C_6$, the pyrimidine-containing strand is visualized by labelling the 3′ end of the *Hin*dIII site. Polylinker DNA fragments containing these triplex target sites were obtained by cutting the plasmids with *Hin*dIII, labelling at the 3′ end using reverse transcriptase and [α-^{32}P]dATP and cutting again with *Eco*RI. The radiolabelled fragments were separated from the rest of the plasmid on 6% polyacrylamide gels.

2.3. DNase I footprinting

15 μl radiolabelled DNA was mixed with 15 μl oligonucleotide, dissolved in 50 mM sodium acetate, pH 5.5, containing 5 mM $MgCl_2$, to give a final concentration between 6–150 μM. Under these conditions the triplex forming oligonucleotides are present at a much higher concentration (> 6 μM) than their duplex target sites (approximately 1 nM strand concentration). As a result the concentration of the third strand remains essentially unchanged throughout the reaction, which approximates to pseudo first-order conditions. 4 μl samples were removed from the reaction mixture at various times after mixing and subjected to short (15 s) digestion with 2 μl DNase I (0.1 units/ml). The reaction was stopped by addition of 4 μl formamide containing 10 mM EDTA. Samples were heated at 95°C for 3 min immediately before electrophoresis.

2.4. Gel electrophoresis

The products of digestion were separated on 9% polyacrylamide gels containing 8 M urea. These were run at 1500 V for about 2 h. Gels were then fixed in 10% acetic acid, transferred to Whatmann 3MM paper, dried under vacuum at 80°C and exposed to autoradiography at −70°C with an intensifying screen. Bands in DNase I digests were assigned

SSDI 0014-5793(94)01387-X

by comparison with Maxam-Gilbert markers specific for guanine or guanine and adenine. Gels were scanned with a Hoefer GS365W microdensitometer. In order to allow for differences in loading and enzyme digestion between lanes, the intensity of bands within the footprint was normalised with respect to a band in the remainder of the fragment. The pseudo first-order rate constant for each reaction (equal to the product of the bimolecular rate constant and the oligonucleotide concentration) was estimated from an exponential fit to the time-dependent data points.

3. Results

Fig. 1 shows the time-dependent appearance of DNase I footprints for the interaction between 5′-Acr-C_5T_5 and a DNA fragment containing the target sequence $G_6A_6 \cdot T_6C_6$. We have previously shown that this short acridine-linked oligonucleotide binds to its target site at low pHs (< 5.5) in the presence of Mg^{2+}, generating parallel $C^+ \cdot GC$ and $T \cdot AT$ triplets [18].

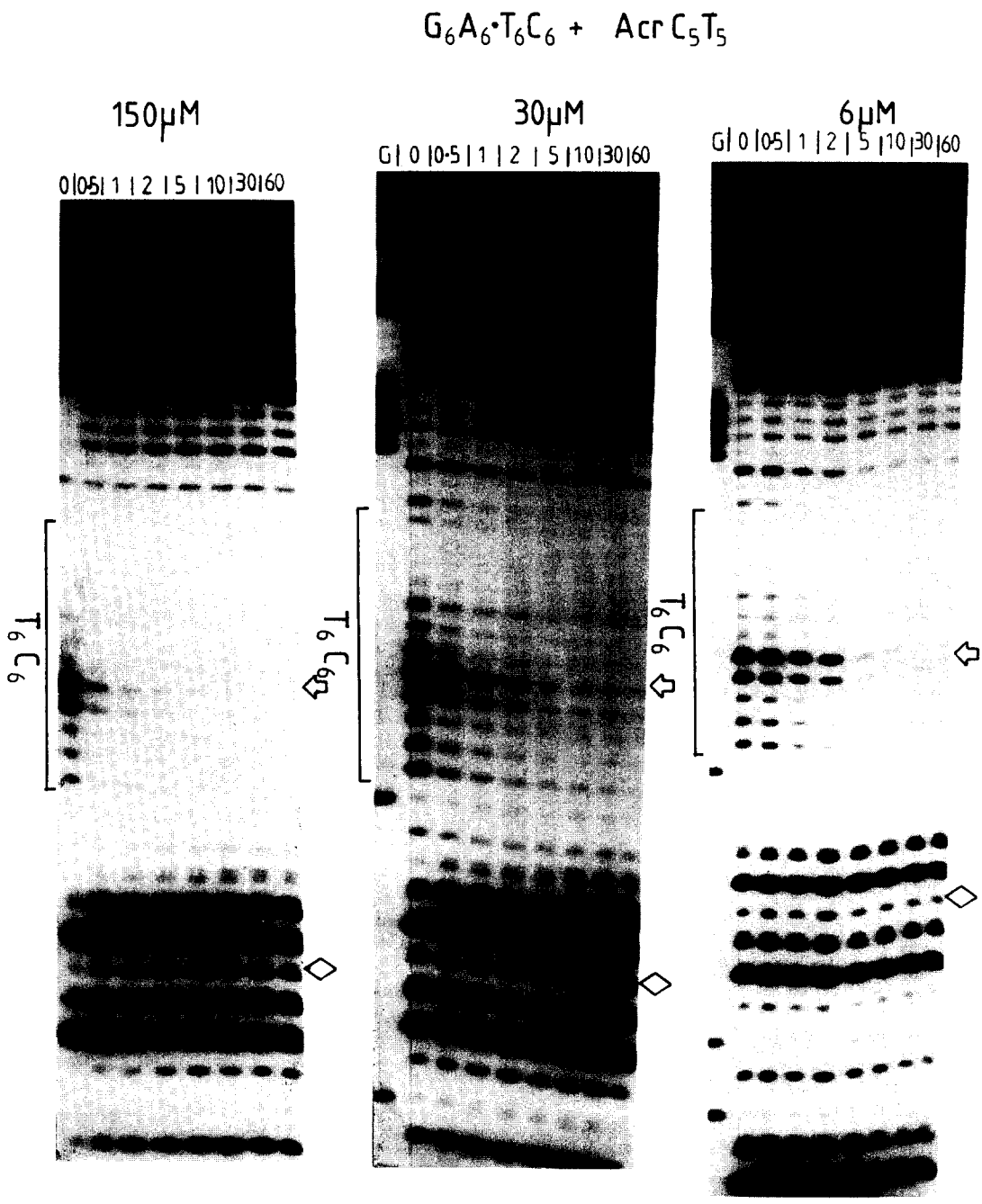

Fig. 1. DNase I digestion patterns showing the association of 5′-Acr-C_5T_5 with a fragment containing the target sequence $G_6A_6 \cdot T_6C_6$, labelled at the 3′ end of the *Hin*dIII site, revealing the pyrimidine-containing strand. The reaction was performed in 50 mM sodium acetate, pH 5.5, containing 5 mM $MgCl_2$. Samples were removed from the association mixture at times indicated at the top of each gel lane (minutes), and subjected to short (15 s) digestion with DNase I. The time 0 lanes correspond to digestion in the absence of added ligand. The oligonucleotide concentration is shown at the top of each panel. The position of the target site is indicated by the square brackets. Tracks labelled 'G' are Maxam-Gilbert dimethylsulphate-piperidine markers specific for guanine. The arrows show the band within the footprint used for the quantitative analysis (Fig. 2). The diamonds indicate the band, outside the footprint, used as a reference for normalising the data.

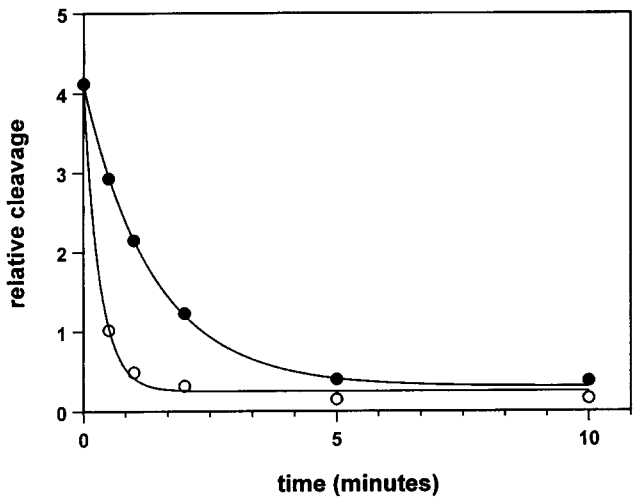

Fig. 2. Quantitative analysis of the interaction of Acr-C_5T_5 with the target sequence $G_6A_6 \cdot T_6C_6$. The points were obtained from a densitometric analysis of the data presented in Fig. 1. The vertical axis shows the intensity of the band indicated by the arrows in Fig. 1, relative to the intensity of a band outside the footprint, indicated by the diamonds. Open and filled circles correspond to 30 μM and 6 μM oligonucleotide, respectively. The curves are expontial fits to the data points with rate constants of 3.15 and 0.74 min^{-1} for 30 μM and 6 μM oligonucleotide, respectively.
←

Looking first at the patterns obtained with 6 μM oligonucleotide it can be seen that the cleavage pattern changes in a time-dependent fashion. 0.5 min after adding the oligonucleotide, the digestion pattern appears the same as that in the control; by 1 min the intensity of bands in the target sequence has decreased slightly; by 5 min the footprint is complete. In this reaction the concentration of the third strand (6 μM) is vastly greater than that of the target site (approximately 1 nM). As a result, the concentration of the free oligonucleotide will be

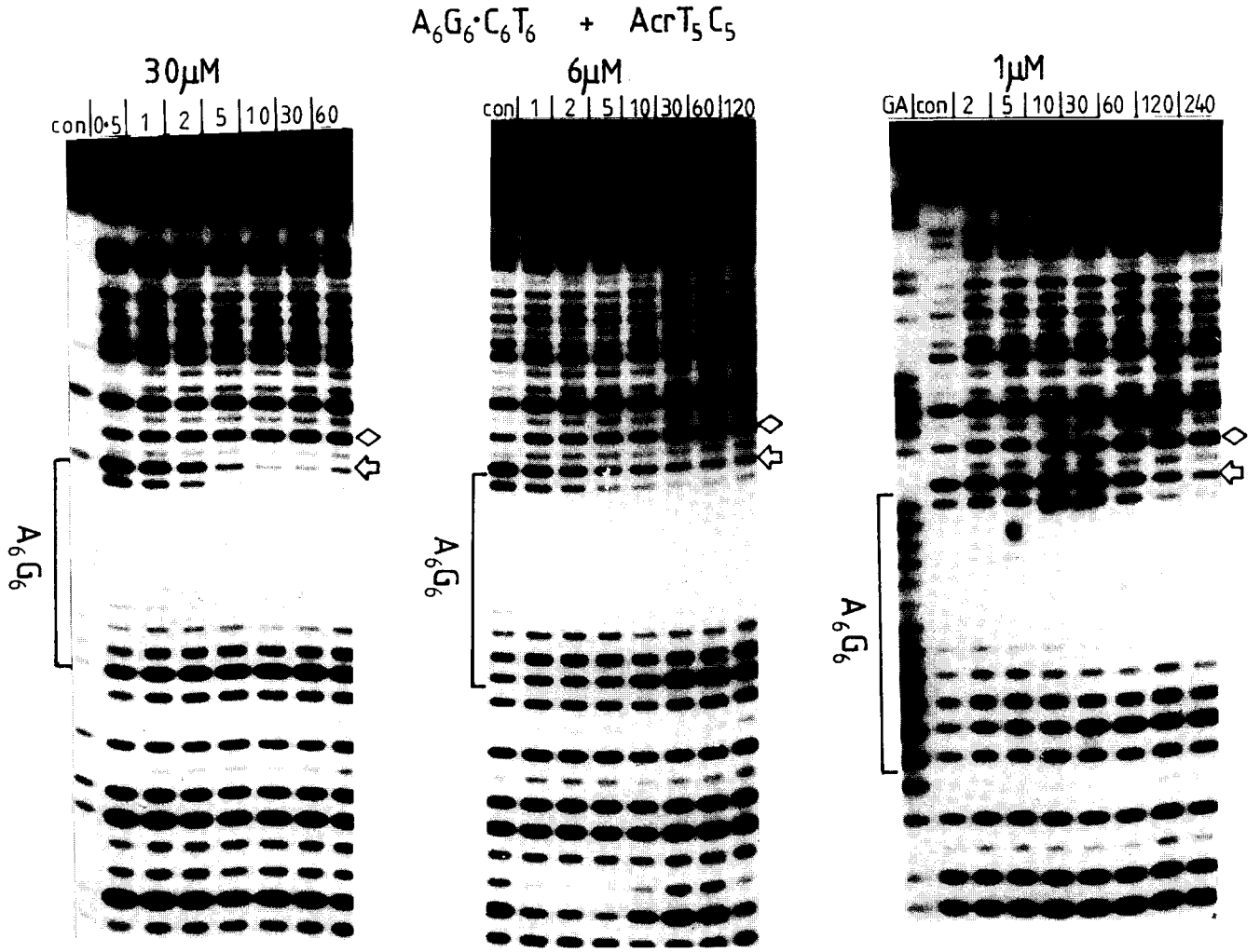

Fig. 3. DNase I digestion patterns showing the association of 5′-Acr-T_5C_5 with a fragment containing the target sequence $A_6G_6 \cdot C_6T_6$, labelled at the 3′ end of the *Hin*dIII site, revealing the purine-containing strand. The reaction was performed in 50 mM sodium acetate, pH 5.5, containing 5 mM $MgCl_2$. Samples were removed from the association mixture at times indicated at the top of each gel lane (minutes), and subjected to short (15 s) digestion with DNase I. 'con' indicates digestion of the DNA in the absence of added oligonucleotide. Bands in the control lane for 30 μM ligand are faint, since this sample is underdigested; the 30 μM patterns are best compared with the control lanes for the lower oligonucleotide concentrations. The oligonucleotide concentrations are shown at the top of each panel. The position of the target site is indicated by the square brackets. The track labelled 'GA' is a Maxam-Gilbert formic acid-piperidine marker specific for purines. The arrows show the band within the footprint used for the quantitative analysis (Fig. 4). The diamonds indicate the band, outside the footprint, used as a reference for normalising the data.

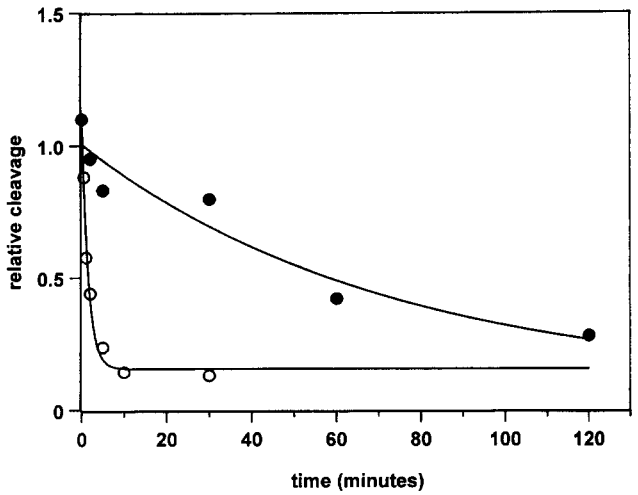

Fig. 4. Quantitative analysis of the interaction of Acr-T_5C_5 with the target sequence $A_6G_6 \cdot C_6T_6$. The points were obtained from a densitometric analysis of the data presented in Fig. 3. The vertical axis shows the intensity of the band indicated by the arrows in Fig. 1, relative to the intensity of a band outside the footprint, indicated by the diamonds. Open and filled circles correspond to 30 μM and 1 μM oligonucleotide, respectively. The curves are expontial fits to the data points with rate constants of 0.65 and 0.014 min^{-1} for 30 μM and 1 μM oligonucleotide, respectively.

essentially unaltered throughout the reaction, which will therefore approximate to a pseudo first-order reaction, with an apparent rate constant k^* given by the product of k_2 (the true bimolecular association rate constant) and the oligonucleotide concentration. If the delayed appearance of the footprint represents a slow bimolecular process then the rate of reaction should depend on the concentration of the oligonucleotide. This is confirmed by the reaction profiles evident with higher oligonucleotide concentrations. With 30 μM oligonucleotide the footprinting pattern is complete between 1 and 2 min, while with 150 μM the reaction is virtually complete by the first time point (30 s).

A more accurate estimate of the association rates can be obtained from densitometric analysis of the data. In order to compensate for differences in the amount of radiolabel in each gel lane, and variations in the extent of enzyme digestion, we have compared the intensity of a band within the footprint (indicated by the arrows in Fig. 1) with a band which is not affected by the presence of the oligonucleotide (indicated by the diamonds in Fig. 1). The results are presented in Fig. 2. Exponential curves fitted to these data points give values for the rate constants of 3.15 ± 0.25 and 0.74 ± 0.02 min^{-1} for 30 μM and 6 μM oligonucleotide, respectively (i.e. half lives of 0.22 and 0.94 min). The reaction with 150 μM oligonucleotide is too fast to obtain a reliable estimate of the rate constant. As expected for a bimolecular reaction, under pseudo first-order reaction kinetics the rate of appearance of the footprints varies in proportion to the oligonucleotide concentration. From these pseudo first-order rate constants ($k^* = [\text{oligo}] \times k_2$) we estimate the bimolecular rate constant to be about 1900 $M^{-1} \cdot s^{-1}$.

We have also examined the rate of formation of short acridine-linked triplexes at a similar target in which the order of G and A bases is reversed, using the sequence $A_6G_6 \cdot C_6T_6$. This is a target for 5′-Acr-T_5C_5, forming a similar complex to the one described above, except that the acridine moiety is now adjacent to the thymines rather than the (protonated) cytosines. We have previously demonstrated that this triplex is stable at pH 5.5 in the presence of Mg^{2+} [17]. Fig. 3 shows the time-dependence of the appearance of DNase I footprints for this interaction. Although this insert is a poor substrate for DNase I, bands at the upper edge are protected from cleavage by the oligonucleotide. Once again it can be seen that the interaction is slow, and can be measured on the footprinting time scale. With 30 μM oligonucleotide the pattern after 1 min resembles that in the control; the footprint becomes apparent between 2 and 5 min. In contrast, with 1 μM oligonucleotide the footprint appears much more slowly and is not evident until after 60 min. Densitometric analyses of the data for 30 μM and 1 μM oligonucleotide are shown in Fig. 4. Exponential curves fitted to these data points yield values for the rate constants of 0.65 ± 0.09 and 0.014 ± 0.011 min^{-1} with 30 μM and 1 μM oligonucleotide, respectively. From these we calculate an average value for the bimolecular rate constant of 300 $M^{-1} \cdot s^{-1}$. This reaction proceeds at about one-sixth the rate of the reaction between Acr-C_5T_5 and $G_6A_6 \cdot T_6C_6$ under identical conditions.

4. Discussion

The results presented in this paper confirm that the rate of formation of intermolecular DNA triple helices is slow, and can be measured on the footprinting time scale. Estimates of the bimolecular rate constants produce values of 300 $M^{-1} \cdot s^{-1}$ for the interaction of Acr-T_5C_5 with $A_6G_6 \cdot C_6T_6$, and 2000 $M^{-1} \cdot s^{-1}$ for Acr-C_5T_5 binding to $G_6A_6 \cdot T_6C_6$. These values are similar to a previous estimate of 10^3 $M^{-1} \cdot s^{-1}$ for triplex formation [11], and suggest that the rate depends on the precise order of the base triplets. However, it is also possible that the differences may be due to the position of the intercalating acridine moiety. In the faster species the acridine is located adjacent to the block of $C^+ \cdot GC$ triplets, whereas it is adjacent to $T \cdot AT$ triplets in the slower species. In this regard it may be significant that polydA·polydT is known to be a poor intercalation site. Unfortunately it is not possible to measure the rate of complex formation with corresponding unmodified oligonucleotides since, under these conditions (20°C), these do not generate clear DNase I footprints [17].

This work demonstrates that the footprinting technique can be successfully employed for measuring the rate of formation of intermolecular DNA triplexes. This technique has several advantages over other kinetic methods in that, not only can the rate of association be visualised directly, but the rate of complex formation can be estimated when the target site is located within a longer DNA fragment.

Acknowledgements: This work was supported by grants from the Cancer Research Campaign and the Biotechnology and Biological Sciences Research Council.

References

[1] Chubb, J.M. and Hogan, M.E. (1992) Trends in Biotechnol. 10, 132–136.
[2] Moffat, A.S. (1991) Science 252, 1374–1375.
[3] Moser, H.E. and Dervan, P.B. (1987) Science 238, 645–650.
[4] Le Doan, T., Perrouault, L., Praseuth, D, Habhoub, N., Decout, J.-L.,Thoung, N.T., Lhomme, J. and Hélène, C. (1987) Nucleic Acids Res. 15, 7749–7760.

[5] de los Santos, C.,Rosen, M. and Patel, D.J. (1989) Biochemistry 28, 7282–7289.
[6] Beal, P.A. and Dervan, P.B. (1991) Science 251, 1360–1363.
[7] Chen, F.-M. (1991) Biochemistry 30, 4472–4479.
[8] Pilch, D.S., Levenson, C. and Shafer, R.H. (1991) Biochemistry 30, 6081–6087.
[9] Blake, R.D. and Fresco, J.R. (1966) J. Mol. Biol. 19, 145–160.
[10] Blake, R.D., Massoulié, J. and Fresco, J.R. (1967) J. Mol. Biol. 30, 291–308.
[11] Maher, L.J., Dervan. P.B. and Wold, B.J. (1990) Biochemistry 29, 8820–8826.
[12] Shindo, H., Torigoe, H. and Sarai, A. (1993) Biochemistry 32, 8963–8969.
[13] Rougée, M., Faucion, B. Mergny, J.L., Barcelo, F. Giovannangeli, C., Garestier, T. and Hélène, C. (1992) Biochemistry 31, 9269–9278.
[14] Wetmur, J.G. and Davidson, N. (1968) J. Mol. Biol. 31, 349–370.
[15] Craig, M.E., Crothers, D.M. and Doty, P. (1971) J. Mol. Biol. 62, 383–401.
[16] Porschke, D. and Eigen, M. (1971) J. Mol. Biol. 62, 361–381.
[17] Stonehouse T.J. and Fox, K.R. (1994) Biochim. Biophys. Acta 1218, 322–330.
[18] Fox, K.R. (1994) Nucleic Acids Res. 22, 2016–2021.